



Droplet_speed-shift keying: a modulation scheme for instantaneous microfluidic communications

Laura Galluccio¹, Alfio Lombardo¹, Giacomo Morabito¹,
Fabrizio Pappalardo¹, Salvatore Quattropani¹⁻²
DIEEI - University of Catania¹
CNIT - University of Catania²
Catania, Italy

ABSTRACT

Microfluidics is a rapidly evolving research area that has attracted the attention of scientists for the huge range of potential applications ranging from medicine to biodefense and drug administration. However to enable the realization of devices that employ droplet microfluidics, efficient and effective methods for encoding information in droplet flows should be identified. So far a number of techniques to encode data have been proposed, e.g., exploiting droplet size, droplet composition, absence or presence of droplets. The above-mentioned methods, however, suffer for the propagation delay inside the channel so that data reception is far from being instantaneous. In fact, a relevant delay can exist in real systems which can be sometimes even in the order of minutes. This occurrence greatly limits the amount of applications that can take advantage of information transmission through microfluidic channels. To try filling the above gap towards a real and prompt deployment of a microfluidic systems, in this paper we propose a novel methodology for encoding information using an instantaneous variation in the properties of a train of droplets flowing in a continuous phase. In particular, taking advantage of the stable, laminar flow of the droplets, we aim to encode data in the instantaneous change of droplet velocity induced by changing the input pressures of the discrete-continuous phases according to the data to be encoded in the source side. This approach opens new perspectives for information transmission in microfluidic systems, which could lead to new applications.

CCS CONCEPTS

• **Applied computing** → *Computer-aided design*.

KEYWORDS

Microfluidics, molecular communications, droplet based communications

1 INTRODUCTION

Molecular Communications promise a plethora of applications in biomedicine [1], [2]. In this context, very interesting opportunities arise, in particular, from the use of microfluidic systems. In fact,

microfluidic channels with a diameter in the order of micrometers can be thought as molecular waveguides[3]. An example of such systems is the Lab-on-a-Chip (LoC), which manipulates small volumes of fluids for chemical and biological analysis and synthesis, with application to controlled drug delivery [4] or diagnostic testing [5]. In this perspective, a new line of research has emerged that combines microfluidics with clinical biology, medicine and physics [6].

Droplet microfluidics allow to manipulate fluids and study certain reactions in controlled environments. The small size of chambers and channels, in the order of micrometers, together with the physical features which derive from the confinement of fluids in such narrow spaces allow several chemical and biological processes to be performed using negligible volumes of liquids [7].

Moreover, in these range of dimensions, molecular consumption is significantly reduced with respect to other traditional macroscale applications. At the microfluidic sizes, capillary forces allow “free” movement of fluids into the channel, but it is necessary to employ one or more pumps to generate and maintain a specific pressure or to add multiple types of reagents into the system [8], [9].

One of the main limitations of state-of-the-art microfluidic systems is that fluids propagate with a very low velocity within the micro-channels. Therefore, in all encoding schemes in which information is tied to each specific droplet, e.g., in droplet content and/or size, the ability to readily receive information is limited by the slowness of droplet movement. This characteristic may represent an inherent limitation to the effectiveness of microfluidic transmission in the case of microfluidic communication systems that must cover non-negligible distance; for example, communication between a microfluidic chip that measures immunoglobulin E (IgE) to detect allergic reactions and a micropump for adrenaline can take up to a minute in the case where they are connected by a microchannel a few tens of centimeters long, which could be incompatible with the need to respond promptly to the occurrence of allergic situations that require a rapid response.

In this work we propose a solution, called *Droplet_Speed Shift Keying* (DSSK) which overcomes the limitations caused by propagation delay inside the microfluidic communication medium. More specifically we encode information in the speed at which a train of drops in a continuous phase moves. By exploiting the stable, laminar flow of the drops, we aim at transferring data throughout the channel almost instantaneously.

The rest of this paper is organized as follows. In Section 2 we introduce some basics on microfluidics, then, in Section 3 we better motivate our work and describe the contribution. In Section 4 we introduce the experimental setup and numerical results are



This work is licensed under a Creative Commons Attribution-NonCommercial-ShareAlike International 4.0 License.

ACM NanoCom 2023, September 20–22, 2023, Conventry, UK

© 2023 Copyright held by the owner/author(s).

ACM ISBN 979-8-4007-0034-7/23/09.

<https://doi.org/10.1145/3576781.3608712>

presented in Section 5. In Section 6 we discuss the relevant open research issues and illustrate future research directions. Finally, in Section 7 we draw our conclusions.

2 BASICS ON MICROFLUIDICS

Molecular communication involves the exchange of information between cells or organisms through the release of signaling molecules, such as hormones or neurotransmitters [10], [11].

In this aim, microfluidic devices offer a powerful platform for investigating the mechanisms and dynamics of molecular communication by enabling precise control on the delivery, on the concentration, and timing of signaling molecules. In addition, microfluidic systems can be used to simulate complex physiological environments, including tissues or organoids [12], [13].

A collection of microchannels with a diameter on the order of micrometers results in the development of a Lab on a Chip (LoC) device. At such scales, immiscible fluids flow in parallel directions, leading to a laminar flow, and fluids are only susceptible to inertia. If such fluids are incompressible, then the microfluidic system is reversible and controllable.

In [14] methods have been established for the measurement of the possible information rates when molecules or other information-carrying particles are utilized in a microfluidic chip. In our previous papers [15],[16] we took a few important steps towards the realization of a microfluidic communication paradigm by adapting conventional communication concepts to the microfluidic domain. These efforts are motivated by the work of Prakash et al. [17] who have shown the feasibility of basic computing using droplets/bubbles [17] and the work of Fuerstman et al. who have shown that communication is possible using droplets in microfluidic channels [18].

Droplet-based microfluidics has been presented as a new method to build programmable LoCs [19, 20]. This novel method involves dispersing a fluid, known as the dispersed phase, into a fluid, known as the continuous phase, which is immiscible with the dispersed phase. With the help of droplet-based microfluidics, it is possible to carry out activities that call for high resolution, sensitivity, and precision by moving samples inside the droplets where each of them can interact with the proper substances under tightly regulated conditions. Droplet microfluidics makes it simpler to regulate samples than continuous-flow microfluidics, which accounts for the growing interest in related techniques. Droplet manipulation with high precision can be achieved via different approaches which exploit electric fields, thermal gradients, magnetic fields, acoustic waves, hydrodynamic forces to drive droplets along the desired direction [19, 21].

Typically a LoC can be utilized for executing a single application, while versatility should be advocated. Instead, the flexibility offered by microfluidic communication capabilities would raise the level of LoCs' competitiveness in a variety of application situations while dramatically lowering the costs of manufacture and development.

In our previous works we have investigated potential methods for information encoding and the corresponding channel capacity [22]; also we have introduced a switching strategy that makes use of signaling data that is encoded in the space between droplets[15]. To control the transport of droplets carrying information and/or chemical and biological samples within microfluidic chips, we introduced

a communication paradigm denoted as Hydrodynamic Controlled Microfluidic Networking [23]. This paradigm solely relies on hydrodynamic microfluidic effects.

Hydrodynamic droplets manipulation actually does not require in-chip electronics and only relies on the use of actuators (pumps and reservoirs) at the edge of the chip.

By introducing the novel idea of bubble logic, some studies have expanded earlier findings on hydrodynamic droplets management in micro-channels [17, 24]. The latter entails using strategically placed bubbles and/or droplets to hydrodynamically direct the flow into a system of tiny channels. Bubble logic enables the implementation of pure hydrodynamic droplets manipulation features in straightforward chips without the need for time-consuming and expensive production procedures.

Whatever is the strategy used to transmit information inside microfluidic channels, delay remains a critical issue that can compromise system reliability and performance due to inherent system limitations (diffusion, friction, pumps settings fluctuations, etc.) [25]. Indeed, despite the efforts made by researchers, the delay in such communication systems is still an unsolved problem.

3 DROPLET SPEED SHIFT KEYING (DSSK)

Modulation is a fundamental technique used in telecommunications to transmit information over long distances. It involves changing the characteristics of a signal, such as its frequency, amplitude, or phase, to encode data within it [26]. This technique allows for the efficient use of the limited frequency spectrum available for communication, as multiple signals can be transmitted simultaneously without interfering with each other [27], [28]. Additionally, modulation provides a degree of security, as encoded signals can be difficult to decipher by unauthorized parties. Modulation techniques have continued to evolve over time, allowing for faster data transmission and more efficient use of communication channels.

In this context, modulation refers to the process of changing/tuning the properties of a fluid, such as its flow rate or composition, in order to encode information. The objective of *droplet speed shift keying* (DSSK) is to exploit the intrinsic physical properties of the microfluidic systems, i.e., the incompressibility and linearity of the flow in an ideal system [29], [30]), to transmit information almost instantaneously over time in a non ideal channel of non-negligible length. This can be achieved by modifying the pressure or fluid mass rate at the inlet of the microfluidic channel. In fact, we expect that as the inlet pressure of the flows varies, an "instantaneous" variation in the speed of the droplets occurs throughout the entire length of the channel immediately. Therefore, DSSK encodes information into the pressure or fluid mass rate at the input of the channel.

Since droplets are formed thanks to the interactions between a flow of the continuous phase and a flow of the dispersed phase, information will be encoded in the variations of the pair of pressures or fluid mass rate of the continuous and dispersed phases. A scheme of the considered modulation scheme is reported in Figure 1.

In the figure, two immiscible fluids, a continuous phase and a dispersed phase are used to generate droplets in a T-junction. The speed of the droplet is controlled by two pumps that input the corresponding phases with appropriate mass flow rates. We call

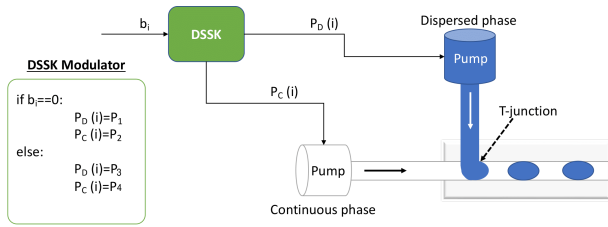


Figure 1: Droplet speed shift keying, DSSK, modulator.

$P_D(i)$ and $P_C(i)$ the mass flow rates of the dispersed and continuous phases, respectively, at the time of transmission of the i -th bit, b_i . More specifically, we assume that $P_D(i)$ is set equal to P_1 while $P_C(i)$ is set equal to P_2 if the bit b_i is 0. Whereas, $P_D(i)$ and $P_C(i)$ are set to P_3 and P_4 if the bit b_i is 1.

The speed of the droplets at the receiver can be detected in several ways. In fact, lasers or cameras can be used. In our experimental setting, as described later in Section 4, we use a pair of lasers and the corresponding photo-receivers.

In order to select the most convenient pairs $P_1 - P_2$ and $P_3 - P_4$, in the following sections we will execute a set of experiments that allow us to find two pairs of pressures values (or mass fluid rates) that result in droplet speeds such that they are not misinterpreted at the receiver. At the same time we want to identify such pairs in such a way that the values $P_1 - P_2$ do not differ too much from $P_3 - P_4$. In fact, in this way the system will be more stable.

Objective of our study is thus to assess the feasibility of the proposed modulation techniques to identify in the most reliable way the current bit being transmitted (bit 0 or bit 1) based only on the observed instantaneous variation of the flow velocity.

4 EXPERIMENTAL SETUP

In this section we describe the experimental setup utilized to assess the feasibility of the proposed approach.

As shown in Figure 2 (upper picture), droplets are generated exploiting a well known microfluidic geometry, i.e., the T-junction. More specifically, the microfluidic chip has been designed using Cinema4D which is a 3D modeling and animation software employed for the creation of complex and detailed shapes. Cinema4D can export the models created in STL format which is compatible with most 3D printing software such as the high resolution Stereolithography (SLA) 3D printing we have then used. The microfluidic chip has a width of 3 cm, a length of 8 cm, and a height of 0.25 cm. Inside the chip, there are two independent and identical rectangular T-junctions with a diameter of $600 \mu\text{m}$ for the dispersed phase channel and $700 \mu\text{m}$ for the continuous phase flow channel (main channel). The fluids are injected into the microchannels using lateral connectors through flexible plastic tubes. The microfluidic chip is characterized by a T-junction angle of 90° , which enhances the stability of droplet formation. The chip has been designed to reduce the occurrence of blockages in the microchannels, which was a common issue in the microfluidic chip employed in [31].

The fluids are injected into the T-junction by exploiting two NE-1002X pumps. They are syringe pumps that use a stepper motor to drive the plunger of a syringe, allowing for precise and controlled

fluid delivery. The NE-1002X has a flow rate ranging between $0.73 \mu\text{L}/\text{min}$ and $10.84 \text{ mL}/\text{min}$, with a maximum pressure of 30 psi. One of them pump oil which will act as the continuous phase, whereas the other will pump colored water. In particular, we used sunflower seed oil purified in water vapor current (Organic Oils S.r.l.) (dynamic viscosity $\mu \approx 0.049 \text{ Pa s}$ and density $\rho \approx 916 \text{ Kg m}^{-3}$) as continuous phase, hereinafter referred to as (Q_o), while water colored blue with food coloring ($\mu \approx 0.001 \text{ Pa s}$, $\rho \approx 1000 \text{ Kg m}^{-3}$) as dispersed phase, hereinafter referred to as (Q_c). No surfactants were added to the two phases.

At the receiver side we needed to measure the velocity of the droplet. To this purpose we designed a system consisting of two laser diodes and two photoreceivers as shown in Figure 2 (bottom picture). The laser diodes we used are two 635nm red laser diodes (Omicron-Laserage Laserprodukte GmbH, LDM635-5), which have a maximum output power of 5 mW and a beam divergence of 0.6 mrad. The lasers are placed 3.5 cm apart and defocus the beam to enable the detection by the light sensor. Two plano-convex optical lenses are placed in between the lasers and the microfluidic circuit to further shape and adjust the beam as needed. The light sensor is an AMBI sensor board with a Sharp GA1A1S201WP light sensor, which is used to detect the defocused laser beam as it passes through the microfluidic circuit. These sensors use a phototransistor to detect changes in the amount of light received when the laser is deflected by the droplets passing through the microfluidic circuit.

Lasers and photoreceivers are controlled by a Arduino board employing the ATmega328P microcontroller.

The output of the photoreceivers has been acquired and processed by a software which we implemented for this work exploiting Node-RED. The software allows to achieve relevant information such as droplet size, space between two droplets, and droplet speed. In our work, Node-RED was used to read data from the light sensor through the serial port at 115200 baud. Processed data was saved in CSV format and displayed on a web-based user interface, providing immediate visual feedback.

5 EXPERIMENTAL RESULTS

In our experiments we have considered the following mass flow rates pairs: 5-3, 8-6, and $10-6 \mu\text{L}/\text{min}$, where the first value refers to the dispersed phase (colored) and the second value refers to the continuous phase (oil).

The measurements were carried out for 3 minutes and repeated in three independent sets of experiments, in order to have a richer dataset and decrease the value of the standard deviation. The global dataset consists of approximately $270 \cdot 10^3$ measurements.

In Figures 3 we introduce three plots. In each of them we show the values of speed measured for several droplets by considering two different pairs of mass flow rates. More specifically,

- in the top plot we show in red the speed values obtained when the mass flow rates are 5 and $3 \mu\text{L}/\text{min}$ and in blue the speed values obtained when the mass flow rates are 8 and $6 \mu\text{L}/\text{min}$;
- in the central plot we show in red the speed values obtained when the mass flow rates are 5 and $3 \mu\text{L}/\text{min}$ and in blue the speed values obtained when the mass flow rates are 10 and $6 \mu\text{L}/\text{min}$;

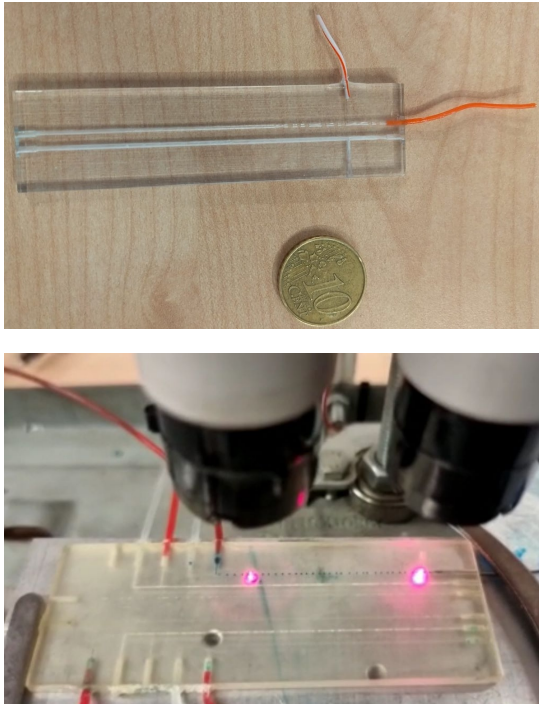


Figure 2: Microfluidic components used in our experiments: T-junction (upper figure) and lasers and photoreceiver (bottom figure)

- in the bottom plot we show in red the speed values obtained when the mass flow rates are 8 and 6 $\mu\text{l}/\text{min}$ and in blue the speed values obtained when the mass flow rates are 10 and 6 $\mu\text{l}/\text{min}$;

In all plots, obviously, on average higher values of speed are measured for pairs with higher mass flow rates (blue markers). We assume that symbol 1 is transmitted by using the pair with higher mass flow rates, whereas the symbol 0 is transmitted by using the pair with the lower mass flow rates.

Therefore, the receiver can distinguish the transmitted symbol by applying a threshold-based demodulation scheme,

- if the droplet speed is higher than the threshold σ_{Th} , then 1 is given as output;
- if the droplet speed is lower than the threshold, σ_{Th} , then 0 is given as output.

In order to identify the most convenient value of the threshold σ_{Th} , we assume that the speed measurements are distributed according to Gaussian distributions each characterized by the mean and variance that we measured in the related experiments. In Table 1 we report the average and standard deviation obtained for each considered pair of mass flow rates.

If this is the case, it is well known that the optimal value of the threshold σ_{Th} is the one in which the probability density functions (pdf's) of the speed for the two pairs have the same value.

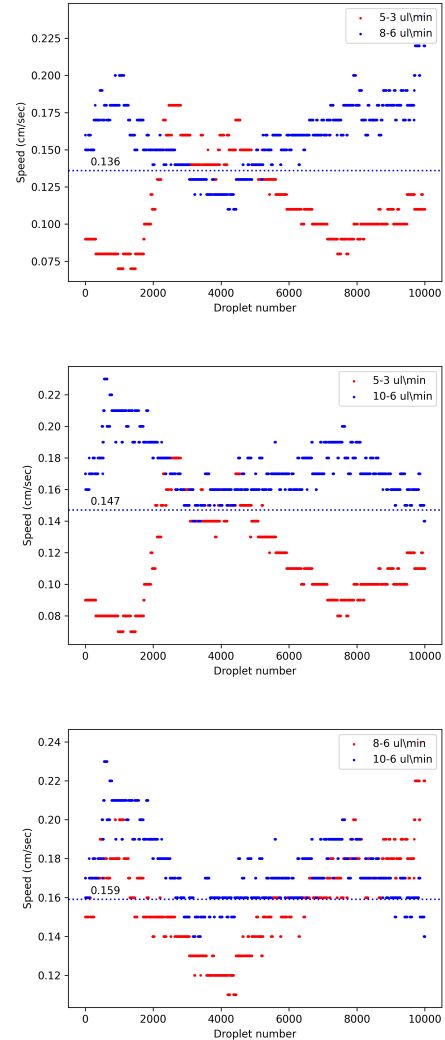


Figure 3: Droplet speed measured at the receiver vs. the droplet sequence number for two pairs of mass flow rates.

Pair	Average	Standard deviation
5-3 $\mu\text{l}/\text{min}$	0.115	0.028
8-6 $\mu\text{l}/\text{min}$	0.159	0.024
10-6 $\mu\text{l}/\text{min}$	0.174	0.018

Table 1: Statistical characteristics of the droplet speeds for different pairs of mass flow rates.

In Figures 4 we show the resulting Gaussian distribution pdfs. More specifically, in each of the three plots we report the pdfs for two pairs of flow mass rates. In particular,

- in the top plot we show in red the pdf when the mass flow rates are 5 and 3 $\mu\text{l}/\text{min}$ and in blue the pdf when the mass

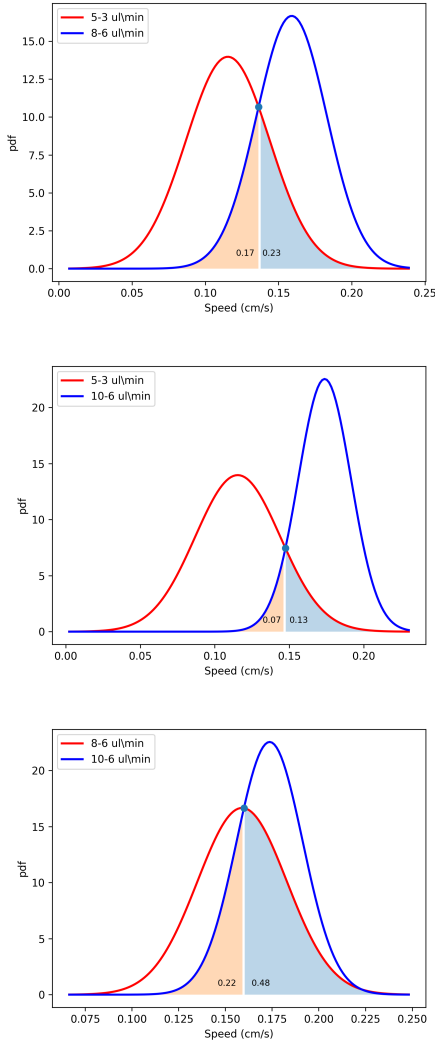


Figure 4: Probability distributions of droplet stream velocities. Each distribution is calculated based on the mean and variance of the dataset, on which a normal distribution is derived.

flow rates are 8 and 6 $\mu\text{l}/\text{min}$. Note that this plot corresponds to the top plot of Figure 3;

- in the central plot we show in red the pdf obtained when the mass flow rates are 5 and 3 $\mu\text{l}/\text{min}$ and in blue the pdf obtained when the mass flow rates are 10 and 6 $\mu\text{l}/\text{min}$. Note that this plot corresponds to the central plot of Figure 3;
- in the bottom plot we show in red the pdf obtained when the mass flow rates are 8 and 6 $\mu\text{l}/\text{min}$ and in blue the pdf obtained when the mass flow rates are 10 and 6 $\mu\text{l}/\text{min}$. Note that this plot corresponds to the bottom plot of Figure 3.

Note that in Figure 4 the values of the threshold, σ_{Th} , to be considered and the corresponding theoretical error probability p_E are those reported in the third and fourth column of Table 2. The values

of the threshold in the three cases are reported in the corresponding plot of Figure 3. By using such values of the thresholds to discriminate the transmitted symbol with the experimental values we have measured the error probability reported in the fifth column of Table 2

Bit 0 pair	Bit 1 pair	σ_{Th}	Theor. p_E	Exper. p_E
5-3 $\mu\text{l}/\text{min}$	8-6 $\mu\text{l}/\text{min}$	0.136	0.2015	0.235
5-3 $\mu\text{l}/\text{min}$	10-6 $\mu\text{l}/\text{min}$	0.147	0.0995	0.0990
8-6 $\mu\text{l}/\text{min}$	10-6 $\mu\text{l}/\text{min}$	0.159	0.351	0.3395

Table 2: Threshold, σ_{Th} , and theoretical and experimental error probabilities, p_E , for different associations between symbols and mass flow rates pairs.

By comparing the error probabilities obtained theoretically and experimentally, as reported in the fourth and fifth column of Table 2, we observe that the predicted, theoretical values of the error probability are enough accurate as the difference with the experimental results is at most 3.35%. Also, we observe that, as expected the maximum error probability is obtained in the case in which the two pressure pairs are closer together, that is, when symbol 0 is encoded with the 8-6 $\mu\text{l}/\text{min}$ pair and symbol 1 is encoded with the 10-6 $\mu\text{l}/\text{min}$ pair; conversely the minimum error probability is obtained in the case in which the two pressure pairs are further apart, that is, when symbol 0 is encoded with the 5-3 $\mu\text{l}/\text{min}$ pair and symbol 1 is encoded with the 10-6 $\mu\text{l}/\text{min}$ pair. Let us observe, however, that a good tradeoff is achieved in the case in which symbol 0 is encoded with the 5-3 $\mu\text{l}/\text{min}$ pair and symbol 1 is encoded with the 8-6 $\mu\text{l}/\text{min}$ pair.

6 LIMITATIONS AND POTENTIAL IMPROVEMENTS

In the proposed microfluidic systems, one of the main challenges is achieving fast response times in order to ensure that the modulation technique is effective. This requires the system to be capable of quickly and accurately changing the fluid properties in response to a signal, as well as detecting these changes with high sensitivity.

One limitation of our proposed system is that the modulation speed is limited by the response time of the pumps used to generate the pressure variations. This means that there is a maximum frequency at which the system can reliably encode information. However, the exact limit will depend on various factors, such as the specific pumps used, the size of the microfluidic channels, and the properties of the fluids being used.

Another factor to consider is the maximum frequency at which the droplets can be generated and detected. This is determined by the physical properties of the fluids and the microfluidic channels, and is related to the maximum velocity at which the droplets can be reliably detected by the lasers.

Despite these limitations, there are many examples of microfluidic systems that are capable of achieving very high modulation

speeds. For example, in the field of automotive fuel injection systems, piezoelectric actuators are used to generate pressure variations with response times on the order of microseconds [32]. Similarly, in the field of inkjet printing, droplets can be generated and manipulated at frequencies of several kHz [33].

Overall, the limitations of our proposed system must be carefully considered when designing and implementing modulation techniques in microfluidic systems. However, with careful optimization of the system parameters, it may be possible to achieve very fast and reliable modulation speeds for a wide range of applications.

7 CONCLUSIONS

In this paper we have proposed Droplet_Speed Shift Keying (DSSK) which is a modulation scheme that can be applied in droplet microfluidic communications to make the delay independent of the channel length. In fact, since fluids are incompressible a variation of the input velocity at the input of a microfluidic channel will (almost) immediately result in a variation of the velocity of the fluid in any section of the microfluidic channel.

In this paper, we have motivated the need for such an approach, we have presented the major characteristics of DSSK and we have presented some preliminary results by exploiting a physical testbed we have realized for the validation of DSSK feasibility.

Experiment results are encouraging, as they demonstrate that it is possible to transmit information through the droplet velocity variation induced by the pressure variation.

8 ACKNOWLEDGMENT

This research is partially supported by the National Operational Plan (PON) Project 4FRAILTY (project code: ARS01_00345).

REFERENCES

- [1] I. F. Akyildiz, F. Brunetti, C. Blázquez, Nanonetworks: A new communication paradigm, *Computer Networks* 52 (12) (2008) 2260–2279.
- [2] W. Guo, M. Abbaszadeh, L. Lin, J. Charmet, P. Thomas, Z. Wei, B. Li, C. Zhao, Molecular physical layer for 6g in wave-denied environments, *IEEE Communications Magazine* 59 (5) (2021) 33–39.
- [3] G. M. Whitesides, The origins and the future of microfluidics, *nature* 442 (7101) (2006) 368–373.
- [4] R. B. Fair, A. Khlystov, T. D. Taylor, V. Ivanov, R. D. Evans, V. Srinivasan, V. K. Pamula, M. G. Pollack, P. B. Griffin, J. Zhou, Chemical and biological applications of digital-microfluidic devices, *IEEE Design & Test of Computers* 24 (1) (2007) 10–24.
- [5] D. Eicher, C. A. Merten, Microfluidic devices for diagnostic applications, *Expert review of molecular diagnostics* 11 (5) (2011) 505–519.
- [6] L. Y. Yeo, H.-C. Chang, P. P. Chan, J. R. Friend, Microfluidic devices for bioapplications, *small* 7 (1) (2011) 12–48.
- [7] N.-T. Nguyen, S. T. Wereley, S. Shaugh, *Fundamentals and applications of microfluidics*, artech house, Inc.: Boston, MA, USA (2006).
- [8] W. Zhao, A. van den Berg, Lab on paper, Lab on a Chip 8 (12) (2008) 1988–1991.
- [9] C. Parolo, A. Merkoçi, based nanobiosensors for diagnostics, *Chemical Society Reviews* 42 (2) (2013) 450–457.
- [10] J. Ozhikandathil, S. Badilescu, M. Packirisamy, Thermally-driven micro-walled nano-composite microfluidic platform for controlled localized surface plasmonic detection of bovine growth hormones, *ECS Sensors Plus* 1 (2) (2022) 023201.
- [11] W. Yao, J. Che, C. Zhao, X. Zhang, H. Zhou, F. Bai, Treatment of alzheimer’s disease by microcapsule regulates neurotransmitter release via microfluidic technology, *Engineered Regeneration* 4 (2) (2023) 183–192.
- [12] Q. Zhong, H. Ding, B. Gao, Z. He, Z. Gu, Advances of microfluidics in biomedical engineering, *Advanced materials technologies* 4 (6) (2019) 1800663.
- [13] V. Velasco, S. A. Shariati, R. Esfandyarpour, Microtechnology-based methods for organoid models, *Microsystems & nanoengineering* 6 (1) (2020) 76.
- [14] N. Farsad, A. W. Eckford, S. Hiyama, Y. Moritani, On-chip molecular communication: analysis and design, *IEEE Trans. Nanobioscience* 11 (3) (2012).
- [15] E. D. Leo, L. Donvito, L. Galluccio, A. Lombardo, G. Morabito, L. M. Zanolì, Communications and switching in microfluidic systems: Pure hydrodynamic control for networking labs-on-a-chip, *IEEE TRANSACTIONS ON COMMUNICATIONS* 61 (11) (2013).
- [16] L. Donvito, L. Galluccio, A. Lombardo, G. Morabito, μ -net: A network for molecular biology applications in microfluidic chips, *IEEE/ACM Transactions on Networking* 24 (4) (2016) 2525–2538.
- [17] M. Prakash, N. Gershenfeld, Microfluidic bubble logic, *Science* 315 (5813) (2007).
- [18] M. J. Fuerstman, P. Garstecki, G. M. Whitesides, Coding/decoding and reversibility of droplet trains in microfluidic networks, *Science* 315 (5813) (2007).
- [19] S.-Y. Teh, R. Lin, L.-H. Hung, A. P. Lee, Droplet microfluidics, *Lab Chip* 8 (2) (2008).
- [20] C.-G. Yang, Z.-R. Xu, J.-H. Wang, Manipulation of droplets in microfluidic systems, *TrAC Trends in Analytical Chemistry* 29 (2) (2010).
- [21] R. Seemann, M. Brinkmann, T. Pfohl, S. Herminghaus, Droplet based microfluidics, *Reports on Progress in Physics* 75 (1) (2012).
- [22] E. De Leo, L. Galluccio, A. Lombardo, G. Morabito, On the feasibility of using microfluidic technologies for communications in labs-on-a-chip, in: 2012 IEEE International Conference on Communications (ICC), IEEE, 2012, pp. 2526–2530.
- [23] L. Donvito, L. Galluccio, A. Lombardo, G. Morabito, Microfluidic networks: Design and simulation of pure hydrodynamic switching and medium access control, *Nano Communication Networks* 4 (4) (2013) 164–171.
- [24] L. F. Cheow, L. Yobas, D.-L. Kwong, Digital microfluidics: droplet based logic gates, *Applied Physics Lett.* 90 (5) (2007).
- [25] G. Fink, A. Grimmer, M. Hamidović, W. Haselmayr, R. Wille, Robustness analysis for droplet-based microfluidic networks, *IEEE Transactions on Computer-Aided Design of Integrated Circuits and Systems* 39 (10) (2019) 2696–2707.
- [26] J. Singh, N. Kumar, Performance analysis of different modulation format on free space optical communication system, *Optik* 124 (20) (2013) 4651–4654.
- [27] G. Woods, P. Papaparaskaeva, M. Shtaif, I. Brener, D. Pitt, Reduction of cross-phase modulation-induced impairments in long-haul wdm telecommunication systems via spectral inversion, *IEEE Photonics Technology Letters* 16 (2) (2004) 677–679.
- [28] M. Lucki, R. Agalliu, R. Zeleny, Limits of advanced modulation formats for transition in fiber optic telecommunication systems to increase speeds from 10, 40, 100 gbps to higher bit rates, in: *Optical Modelling and Design III*, Vol. 9131, SPIE, 2014, pp. 591–599.
- [29] Y. Dou, B. Wang, M. Jin, Y. Yu, G. Zhou, L. Shui, A review on self-assembly in microfluidic devices, *Journal of Micromechanics and Microengineering* 27 (11) (2017) 113002.
- [30] T. M. Squires, S. R. Quake, Microfluidics: Fluid physics at the nanoliter scale, *Reviews of modern physics* 77 (3) (2005) 977.
- [31] L. Donvito, L. Galluccio, A. Lombardo, G. Morabito, A. Nicolosi, M. Reno, Experimental validation of a simple, low-cost, t-junction droplet generator fabricated through 3d printing, *Journal of Micromechanics and Microengineering* 25 (3) (2015) 035013.
- [32] R. S. Wijetunge, C. J. Brace, J. G. Hawley, N. D. Vaughan, R. W. Horrocks, G. L. Bird, Dynamic behaviour of a high speed direct injection diesel engine, *SAE Transactions* 108 (1999) 1120–1129. URL <http://www.jstor.org/stable/44743442>
- [33] P. Cooley, D. Wallace, B. Antohe, Applications of ink-jet printing technology to biomed and microfluidic systems, *JALA: Journal of the Association for Laboratory Automation* 7 (5) (2002) 33–39.